ISSN 2229-5518

Development of nano-grained Calcium Hydroxyapatite using slip casting technique

Howa Begam, Abhijit Chanda and Biswanath Kundu

Abstract— The purpose of this study is to synthesize nano-grained Calcium Hydroxyapatite (HAp) through slip casting technique. For this, hydroxyapatite powders were synthesized using two methods, wet chemical method and Ammoniacal method. The as-prepared powders and calcined powders were characterized using XRD, FTIR, to study the phases of the powders. The hydroxyapatite powder calcined at 1000°C for 2hr was used to prepare 50 vol% slurry using DN40 (sodium polyacrylate) as dispersing agent. After slip casting, the green bodies were sintered at different temperatures, 1100, 1200, 1250 and 1300°C with 2hr soaking time. The sintered dense samples were characterized for physical, mechanical and biological behavior.

Key Words – Slip casting, Hydroxyapatite, Ammoniacal method

1 INTRODUCTION

CALCIUM phosphate ceramics, mainly Hydroxyapatite (HAp), do not exhibit any cytotoxic effects, shows excellent biocompatibility with hard tissues and also with skin and muscle tissues, and is the most appropriate ceramic material for hard-tissue replacement. This is a bio-active material with wide range of applications ranging from bone replacement to controlled drug delivery system. Albee (1) reported the first successful medical application of calcium phosphate bioceramics in humans, and in 1975 Nery et al. (1) reported the first dental application of these ceramics in animals. Since then, lot of work has been done on the in-vivo performance of Hap (2,3). But the applications of pure HAp are limited due to its poor mechanical reliability. Though HAp is generally used for replacement of different types of bones, it can not be used for load bearing situations. In recent past, much work has been done towards the development of advanced processing techniques for achieving more functionally reliable bioceramic bodies. Refinement of grains (4), advancement in sintering process through microwave (5), doping with various ions (6-8) are some of the approaches adopted so far for improving the mechanical strength of this group of bio-ceramic materials. Due to high surface energy, nano-sized HAp powder results in better sinterability and therefore improves mechanical properties. For this reason, researchers have developed many HAp synthesis techniques, including sol-gel methods (8,9), co-precipitation (10), emulsion techniques(11), mechano-chemical methods (12), electrochemical deposition (13), and hydrothermal processes (14). Colloidal processing can also be a promising technique to achieve this objective.

In colloidal processing, particle dispersion is the most important factor, which has a strong influence on both the rheology and homogeneity of the suspensions. Various colloidal processes, such as slip casting (15), tape casting (16) and gel casting (17,18) etc. have been reported for preparation of HAp with different size and complicated shapes. It has been shown that anionic polyelectrolyte is very effective to obtain homogeneous distribution of HAp particles. M. Toriyama et al (18) investigated the dispersion behavior of mechanochemically synthesized hydroxyapatite. They showed that surface charge reversed as anionic polyelectrolytes were added in considerably high amount (3 wt%). It was further shown that polyacrylates were effective in stabilizing 10 vo1% suspensions while pourable casting slips were obtained at the maximum solid concentration of 21.4 vol %. Rao et al (15) studied the dispersibility of HAp in deionized water using sodium hexametaphosphate and ammonium polymethacrylate as dispersing agent.

In the present work, Hap powder was prepared by two methods- wet chemical and ammoniacal route method. These powders were characterized by different tools and slips were prepared with different concentration of dispersant to optimize the slip viscosity ideally suited for slip casting. Sinterability of these slip cast samples and their physical, mechanical and biological characterization have been performed.

2 MATERIALS AND METHOD

Hydroxyapatite powders were synthesized using two methods- wet chemical route and Ammoniacal route. In wet chemical method, G.R. calcium hydroxide ($Ca(OH)_2$) and orthophosphoric acid (H3PO4)(EMerck,India) were used. H_3PO_4 solution was added drop by drop in the $Ca(OH)_2$ solution in stirring condition. Synthesis was done at 80°C at a pH of 11-12. In ammoniacal method, A.R. grade Calcium Acetate ($(CH_3COO)_2Ca.XH_2O$) and

L.R. grade (Ammonium phosphate Di basic) ($(NH_4)_2HPO4$ NICE Chemicals Pvt. Ltd, India) were used. Aqueous solution of ammonia and Di Ammonium hydrogen orthophosphate were added drop by drop to the aqueous solution of Calcium Acetate with continuous stirring at 80˚C. After 48 hours, the precipitate was filtered and washed continuously with distilled water to remove ammonia. The as-prepared powders were then calcined at 1000°C for 2hr. Samples prepared with wet chemical method were designated with the name URH while those prepared via Ammoniacal route were termed as ARH.

The calcined powders were planetary milled in ethanol medium with 50 rpm for 3hr to gain suitable particle size distribution and specific surface area. The particle size distribution was measured using laser diffraction technique in Mastersizer instrument (Malvern Instruments Ltd., UK) and the specific surface area was measured by BET method (Sorpty 1750, Italy). The phase composition of as prepared powder and calcined powder was analyzed by X-ray diffraction (XRD, Cu Kα1, Philips Analytical, PW1710, Netherlands). FTIR analysis was made in mid IR region (4000-400 cm-1) using KBr pellets in a Perkin-Elmer, Model 1615 (USA) instrument. The differential thermal analysis and thermo gravimetric analysis was done for as prepared powders using DTA/TGA instrument (NETZSCH, Germany),

An anionic polyelectrolyte with trade name Dispex N 40 (DN40) was used as deflocculating agent to prepare HAp slip. To optimize the amount of DN40 to be added, zeta potential of HAp- loaded slip was measured with different concentration of DN40 (0 - 5wt %) and with varying pH. It was performed in Zetasizer instrument (Malvern Instruments Ltd., UK). The slurry was planetary milled for 16 hours to obtain homogeneous solution. The rheological behavior of the aqueous suspensions of HAp powder (40-50 vol %) was studied with varying shear rate from 0 – 450/s using a cup-and cone arrangement (HAAKE, VT500 with sensor-5 mode) at room temperature with about 50% relative humidity.

HAp slurry with a maximum volumetric load of 50% was finally used for slip casting. It was done in a Plaster of Paris mould with 40-50 % porosity to prepare dense Hap. Sinterability of the dense HAp was studied in an electrical resistance furnace (Naskar Furnace, Kolkata, India) at different temperatures 1100, 1200, 1250 and 1300˚C with 2 hrs dwelling time for each. The heating rate was kept constant for all the cases at 3˚C/min. After cooling, the sintered samples were cut in different shapes for physical, mechanical and biological characterization.

The bulk density and porosity of the sintered samples were measured using water displacement method which is based on Archimedean principle. After taking the weight of the dried samples (D), they were soaked in water to get soaked weight (W). Weight of the samples in water-suspended condition (S) was also measured. Density, open and closed porosity were calculated using standard expressions as mentioned below.

Bulk density (B.D.) = D/(W-S) gm/cc, Apparent Porosity (A.P.)= (W-D)/(W-S) x100%

Total Porosity (T.P.) = (1-B.D./True Density) x100%, Closed Porosity (C.P.) = T.P.-A.P. True density of HAp was 3.167g/c.c. The phases of sintered HAp samples were identified by X-ray diffractometry (XRD, Cu Kα1, Philips Analytical, PW1710, Netherlands). Scans were recorded from diffraction angle (2θ) of 10° -80°, at a speed of 40/min with step size of 0.050. The surface morphology as well as the microstructure of the dense samples were observed to assess the influence of the sintering temperature on the grain size of hydrxyapatite, by using a Scanning Electron Microscope (S3400N, Hitachi).

Young's modulus and hardness was calculated from the nanoindentation technique (CSM, Switzerland), at a load of 100mN for both ARH and URH samples using standard Oliver and Pharr technique. Bi-axial flexural strength and compressive strength was also measured using a Universal testing machine (Instron 5500R, UK).

Cell adhesion behavior was studied for the HAp pellets at Shree Chitra Tirunal Institute for Medical Science and Technology, Kerala, India. L929 mouse fibroblast cells were seeded on the surface of conditioned HAp samples with minimal essential medium supplemented with 10% fetal bovine serum, 100 units/ml of penicillin and 100 μg/ml streptomycin, respectively and incubated at 37°C in humid atmosphere and 5 % CO2 for 48 hours.

3 Results and Discussion

Various results of physical, mechanical and biological studies are presented and discussed below. The XRD was performed on as prepared powder as well as the calcined powder. It has been found that as prepared URH powder consists of phase pure hydroxyapatite with the major peak at 31.8 degree (Fig 1a). When the same powder was calcined at 1000˚C minor quantities of secondary phase viz. calcium oxide appeared (Fig. 1b).

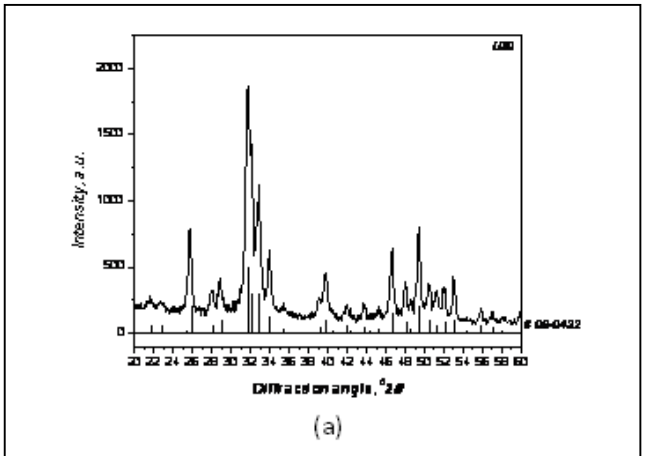

(a)

Fig. 1a. XRD pattern of URH

This may due to the degradation of Hydroxyapatite at that temperature and at that atmospheric pressure. After slip casting using this powder, the dense blocks were fired at 1100˚C, 1200˚C,1250˚C, 1300˚C and it was found that calcium oxide was retained as minor quantities up to the temperature as high as 1300˚C.

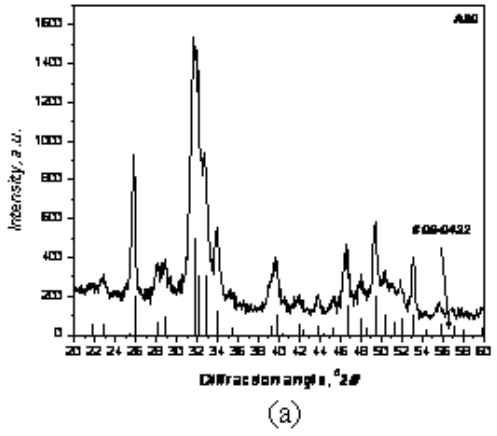

(a)

Fig: 2a XRD pattern of ARH

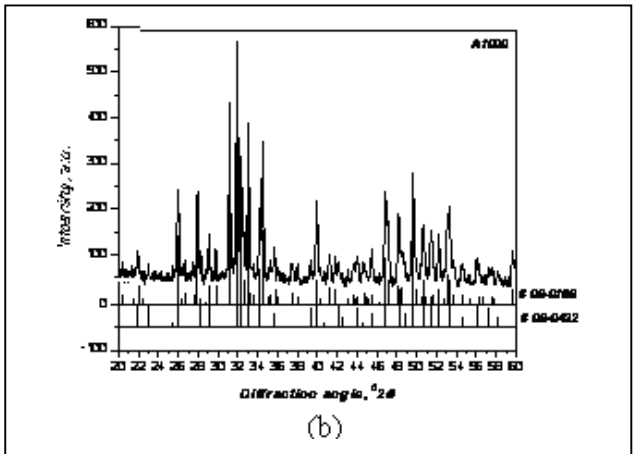

(b)

Fig: 2a XRD pattern of ARH

Similarly the as prepared ARH powder was composed of phase pure Hydroxyapatite (Fig 2a). When the same powder was fired for calcination at 1000˚C some part of Hydroxyapatite decomposed to form another crystalline phase which is β-TCP (Fig 2b). It was found that percentage of β-TCP went on increasing from the temperature 1100-1300˚C.

Average crystallite size is calculated from the XRD of as prepared powder as well as the sintered slip casted dense blocks sintered at different temperatures using by using Full Width at Half Maxima (FWHM) method. It was based on Scherrer's equation i.e., $D=0.9\ \lambda/\beta\cos\theta$ where, D=size of the crystal, λ=wavelength of X-ray used, β=broadening of diffraction line at half of its maximum intensity in radians, θ =diffraction angle.

The average crystallite size of URH increases with increase in temperature upto 1200 ˚C. After this temperature the crystallite size decreases. For ARH the crystallite size went on increasing up to temperature of 1100˚C for c Axis of Hydroxyapatite. It was not the case for the plane (300). The dimension of a axis went on increasing up to a temperature as high as 1250˚C.

Percentage of crystallinity of powder and dense block were calculated by using the following relationship :

$X_C = (1- V_{112/300} / I_{300})$

where, V112/300 is intensity of hollow between the planes (112) and (300) reflections and I300 is the intensity of (300) reflection. It was found that for URH powder and sintered blocks percentage of crystallinity went on increasing up to temperature of 1200˚c. After that it was decreasing up to 1300˚c possibly due to presence of minor quantity of CaO.

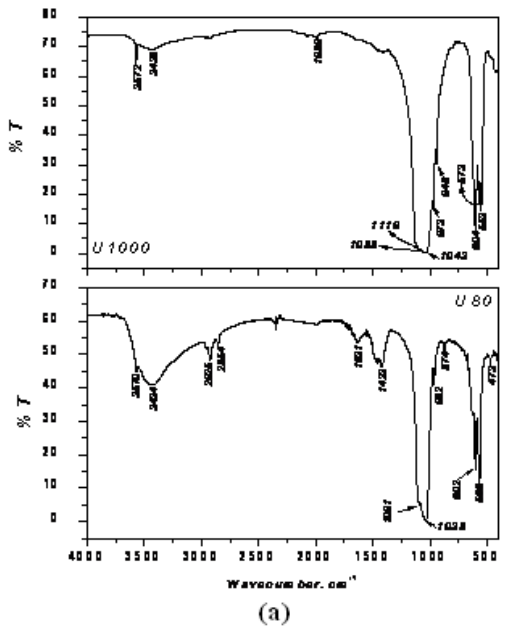

(a)

Fig. 3a. FTIR spectra of As prepared and sintered URH powder

The crystallinity calculated from ARH1000 powder was found to be highest which drastically decreased at 1100˚C and subsequently went on increasing upto 1250˚C.

In FTIR plot for as prepared ARH, bulge shaped peak at 3436 was found which reveals the presence of hydroxyl group. In the A1000 (ARH sintered at 1000˚C) plot this hydroxyl group peak is very short and tending to disappear. This might be due to the evaporation of the surface moisture of the powder for calcination. In A1000 the presence of peaks at 973, 963, and 947 reveals the presence of TCP. So from the FTIR plot too, evidence regarding the conversion of hydroxyapatite into TCP was obtained. The hydroxyl group was also present in as prepared URH like

ISSN 2229-5518

ARH. In U1000 (URH sintered at 1000C) the hydroxyl group is trying to disappear this may due to the evaporation of the surface moisture of the powder after calcinations.

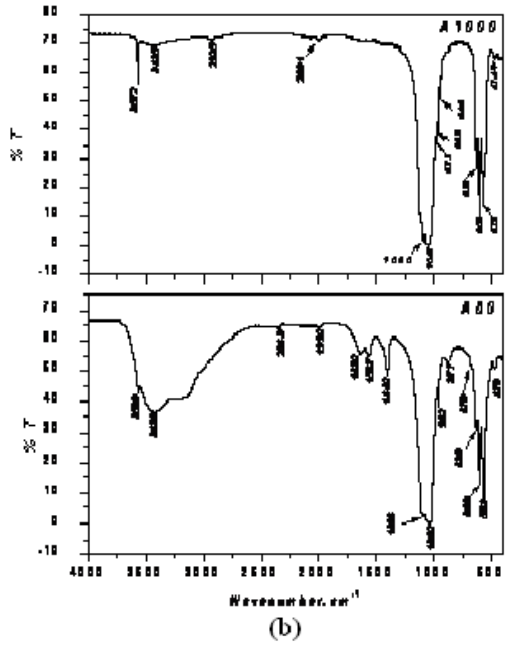

(b)

Fig. 3b. FTIR spectra of As prepared and sintered ARH powder

The surface morphology as well as the microstructure of the dense samples was observed to assess the influence the sintering temperature on the grain size of hydroxyapatite by using scanning electron microscope. It was observed that for both the type of Hap, samples sintered at 1100˚C had homogeneous microstructure and grains were more or less uniform and fine. In high sintering temperature the microstructure changed and grain size increased for both the type of hydroxyapatite samples. Average grain sizes were 213 ± 64 nm, 438.92 ± 110.612 nm, 797.51 ± 156.3546 nm and 1.56 ± 0.288 micron respectively for URH samples sintered at 1100, 1200, 1250 and 1300˚C. For ARH samples average grain sizes were 213 ± 53 nm, 851 ± 118 nm, 1073 ± 216 nm and 2136 ± 441nm for samples sintered at 1100, 1200, 1250 and 1300C respectively.

The specific surface areas in m2/gm for all samples were listed in the table.

TABLE:1

THE SPECIFIC SURFACE AREAS FOR ALL SAMPLES

Samples	Specific surface area, (m2/gm)
ARH(as prepared)	77.284
URH (as prepared)	40.843
ARH 1000	2.583
URH 1000	20.439

It reveals that calcined URH powders had higher specific surface area than ARH. Specific surface area played an important role for slurry stabilization and it was not possible to achieve high solid loading for higher specific surface area [19]. The specific surface area obtained was lower which made the slurry high solid content.

The median size of the URH before milling was 8.64 micron. Before milling the particle formed agglomerate. After milling the powder median size decreased and was subsequently was used for slip casting. The particle size distribution curve was a bimodal curve. We got two values for median size 1.61 and 4.92 micron. It was known that particle size around 2 microns is ideal for slip casting. The curve showed the presence of even smaller particles in the present case. In case of ARH before milling, the particle size distribution curve was a bimodal curve but after milling the curve had a fine Gaussian peak. The median size was 2.90 micron, not much different from the ideal one and hence suitable for slip casting.

Variation of surface charge with varying amount of percentage of dispersant for aqueous suspension of both URH1000 and ARH1000 particle were measured which is given in fig(4). It was found that with addition of dispersant, URH particles became highly deflocculated and the trend was continued up to 5wt%. For a particular aqueous suspension of powder particles it is known that the value of zeta potential anything between35 to 50 mV should have higher deflocculating properties. The same trend was observed for URH particles. From the plots it could be inferred that 4-5 wt% DN40 had the ability for idealized dispersion of URH1000 particles. In case of ARH, zeta potential values had a different behavior with addition of dispersant. In this case, the zeta potential values were found to be very high with the addition of DN40 from 1-4 wt %. So any quantities between these ranges may show high dispersion in the aqueous system of ARH1000 particles. After addition of 4% DN40 the particles started to agglomerate and continued up to 5wt%. So finally 4% of DN 40 was selected for effective defloculation.

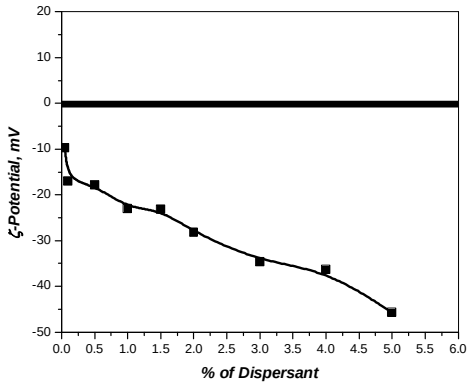

Fig. 4a. Surface charge with varying amount of DN40 of URH

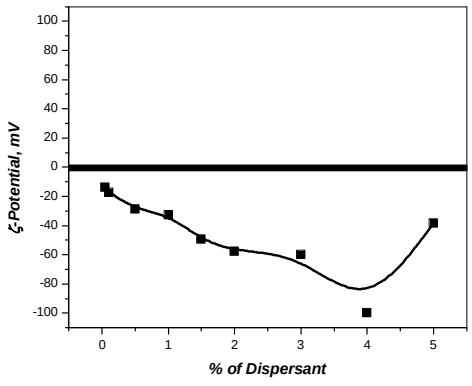

Fig. 4b. Surface charge with varying amount of DN40 of ARH

Changes of viscosity (expressed as mPa.-s) and shear stress for both URH and ARH particles with varying amounts of solid loading. It has been found that the slurries behaved like a Bingham plastic for the total range of shear rates. The behavior was more prominent for 50 vol% slurry where it was found to be almost a straight line having a y-axis intercept.

The bulk density was measured by water displacement method that employs Archimedes's principle. The figure (5) shows the variation of bulk density with sintering temperature. It was observed that bulk density increases with increase in sintering temperature for both URH and ARH samples and the bulk density was maximum at 1250˚C as shown in the figure. For ARH samples sintered at 1250˚C maximum density was obtained which was 97.56% of actual density. For URH samples we observed the same thing like ARH i.e. density increase with increase in sintering temperature. We got the maximum density 93.3% of actual density for URH1250. It was observed that URH and ARH samples sintered at 1100˚C have more apparent porosity but the closed porosity is less compared to other samples. The apparent porosity and closed porosity for ARH 1200, ARH1250 and ARH1300 were more or less same.

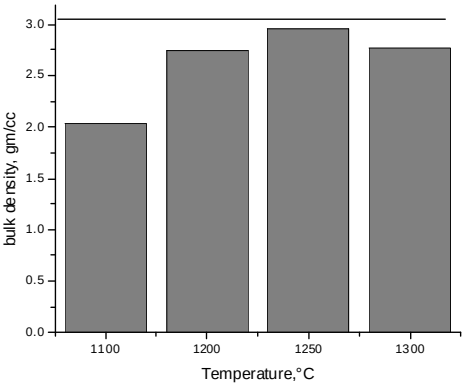

Fig. 5a.Sintering temperature versus bulk density of URH

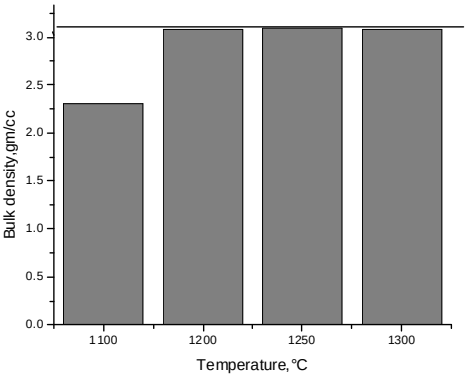

Fig. 5b.Sintering temperature versus bulk density of ARH

Vickers' hardness and nano indentation hardness was measured for both URH and ARH blocks sintered at 1100˚C and 1250˚C. It was found that URH1250 had more Vickers' hardness value (4.23GPa) than URH1100. Same results was observed for ARH 1250 i.e. Vickers' hardness value for ARH1250 was 4.14GPa which is better than ARH1100. The hardness obtained from nano-indentation showed more or less a similar trend like Vickers' hardness. The flexural strength was measured for both URH and ARH blocks sintered at 1100˚C and 1250˚C. The flexural strength of URH1250 and URH1100 were 94.01 MPa and 18.99 MPa respectively. For ARH1250 and ARH1100 the average flexural strength was obtained as 67.32 MPa and 38.04 MPa respectively. For flexural strength as well as hardness, the individual scatter was well within 5%. For both URH and ARH, at 1100C, the materials were found to be too porous. Drop in hardness or flexural strength for both URH and ARH at 1100˚C might be attributed to this increased porosity. It may be

noted that the samples sintered at 1100˚C with a soaking time of 2 hrs consisted of nano grain size but due to porosity their mechanical properties degraded. In case of compressive strength, however this was not followed in an identical manner in case of ARH. The exact reason behind it was not clear but in this case (1250˚C) three samples were tested and the results showed large (more than 100%) scatter. The values varied widely from 13.82 MPa to 152.19 MPa while in 1100˚C, with same number of specimens, the standard deviation was substantially lower, 22%. This might have caused some discrepancy in the general trend of lower mechanical property at 1100˚C.

Fig. 6a.SEM micrograph of cellular adhesion URH blocks sintered at 1200°C/2hrs

Fig. 6b.SEM micrograph of cellular adhesion ARH blocks sintered at 1200°C/2hrs

Cell-material interaction plays a very vital role in case of bioactive ceramics. In the present case, L929 mouse fibroblast cells were used to study the cell adhesion on the hydroxyapatite blocks sintered at 1250˚C for 48 hrs. The time of the study was short due to some machine constraints. It was observed that preliminary fibroblast cell adhesion on URH was better than ARH samples. Although in URH, the number of cells attached to the surface was not high, the primary signs of extending filopods clinging to micro-structural anchorage sites were observed. Such behavior was not found in ARH even after thorough scanning throughout the surfaces. It might be due to the presence of secondary phase (β-TCP) in ARH samples that did not promote cell attachment, cell growth and spreading capability like the other case. β-TCP are reported to affect the microenvironment of the cell culture [3] by leaching ions and changing the pH of the medium resulting in an unstable interface which prevent proper anchorage; attachment and adhesion in an acidic medium.

From the results discussed so far, it is evident that nano-sized hydroxyapatite was synthesized in a very simple and economical way of slip casting method without sacrificing the quality of the product. It has been observed that if suitable deflocculating process is adopted following thorough study of rheological behavior of the slip, casting of dense pellets are possible with consistent microstructure and compositional homogeneity. It is an accepted fact that grain refinement increases strength according to Hall and Petch [20,21] but porosity in the nano grained sample, can classically cause deterioration of mechanical strength. The present material was nano-grained with porosity as high as 30%. This was found for both URH and ARH HAp at 1100˚C. The values were found not only from density measurement but also from image analysis. Furthermore the pores were found to be grossly interconnected which is ideal for in-vivo bony in growth and osteointegration.

Normally cortical bones have compressive strength in the order of 100-130MPa and hardness around 1-2 GPa. To verify a set of tests were conducted with human cadaveric bones (both male and female cortical bones) with same test set-ups as used here in case of HAp. The compressive strength values in axial direction were in the order of 150 MPa while hardness was less than 1 GPa. Here at 1100C, the maximum value of compressive strength we got for ARH was slightly less than 100 MPa, however hardness was comparatively high, around 3.11 GPa. So for load bearing implant this type of porous material might not be generally recommended right now from mechanical point of view. But this porosity would be advantageous for non-load bearing implants where cells could attach with high number of anchorage sites. This enhanced attachment could trigger other associated activities differentiation and proliferation.

4 CONCLUSION

Nano sized hydroxyapatite could be successfully synthesized using two co-precipitation methods. Submicron and/or nano ranges of grain size of Hydroxyapatite could be consistently formed by slip casting method using high deflocculated suspension of

URH & ARH. It was confirmed by the SEM, BET and particle size distribution study. Highly deflocculated suspension was prepared successfully for both the powders. Solid loading as high as 50 vol% could be achieved using an acrylic based anionic dispersant. This was correlated with the findings of assessment of zeta potential with varying amount of dispersant addition. The slip casted blocks were sintered at fairly low temperatures with > 95% density. URH 1250 showed highest values of hardness and Young's modulus as calculated from both Vickers indentation and nano indentation. Fibroblast cells adhesion on URH was better than ARH. Slip casting is very effective and efficient method to get fine grained hydroxyapatite.

REFERENCES

[1] R.Z. LeGeros, 40th Symposium on Basic Science of Ceramics, Convention Center, Osaka University, January 22–23,

[2] A.Banerjee, A. Bandyopadhyaya, S.Bose, W. M. Keck, Hydroxyapatite nanopowders: Synthesis, densification and cell–materials interaction, Materials Science and Engineering C 27 (2007) 729–735

[3] Annie John, H. K. Varma & T. V. Kumari, Surface Reactivity of Calcium Phosphate Based Ceramics in a Cell Culture System, Journal of biomaterial applications, V-18 (2003)

[4] Samar J. Kalita , Abhilasha Bhardwaj, Himesh A. Bhatt, Nanocrystalline calcium phosphate ceramics in biomedical engineering, Materials Science and Engineering C 27 (2007) 441–449

[5] I. Teoreanu , M. Preda , A. Melinescu, Synthesis and characterization of hydroxyapatite by microwave heating using CaSO4_2H2O and Ca(OH)2 as calcium source, J Mater Sci: Mater Med (2008) 19:517–523

[6] S. J. Kalita, D. Rokusek, S. Bose, H. L. Hosick, A. Bandyopadhyay, Effects of MgO-CaO-P2O5-Na2O-based additives on mechanical and biological properties of hydroxyapatite, 2004 Wiley Periodicals, Inc.

[7] S. J. Kalita, D. Rokusek, S. Bose,1 H. L. Hosick, A. Bandyopadhyay , CaO–P2O5–Na2O-based sintering additives for hydroxyapatite (HAp) ceramics, Biomaterials 25 (2004) 2331–2339

[8] A. Bandyopadhyay , Elizabeth A. Withey, J. Moore, S Bose, Influence of ZnO doping in calcium phosphate ceramics, Materials Science and Engineering C 27 (2007) 14–17

[9] A.H. Rajabi-Zamani, A. Behnamghader, A. Kazemzadeh Synthesis of nanocrystalline carbonated hydroxyapatite powder via nonalkoxide sol–gel method, , Materials Science and Engineering C (2008)

[10] Y. X. Pang and X. Bao, Influence of temperature, ripening time and calcination on the morphology and crystallinity of hydroxyapatite nanoparticles, J. Eur. Ceram. Soc.(2003) 1697.

[11] G. K. Lim, J. Wang, S. C. Ng, C. H. Chew and L. M. Gan, processing of hydroxyapatite via microemulsion and emulsion routes, Biomaterials18 (1997) 1433

[12] W. Kim, Q.W. Zhang, F. Saito, Mechanochemical synthesis of hydroxyapatite from Ca(OH)2–P2O5 and CaO–Ca(OH)2–P2O5 mixtures, J. Mater. Sci. 35 (2000) 5401–5405.

[13] L.Y. Huang, K.W. Xu, J. Lu, A study of the process and kinetics of electrochemical deposition and the hydrothermal synthesis of hydroxyapatite coatings, J. Mater. Sci. Mater. Med. 11 (2000) 667.

[14] Jae-Kil Han, Ho-Yeon Song, Fumio Saito, Byong-Taek Lee, Synthesis of high purity nano-sized hydroxyapatite powder by microwave-hydrothermal method, Materials Chemistry and Physics 99 (2006) 235–239

[15] R. Ramachandra Rao and Thandali S. Kannan , Dispersion and Slip Casting of Hydroxyapatite, J.Am.Ceram.Soc.84[8] 1710-16(2001)

[16] I.H. Arita, D.S. Wilkinson, V.M. Castazo, Synthesis and Processing of Hydroxyapatite Ceramic Tapes Casting with Controlled Porosity J. Mater. Sci. Mater. Med. 6 (1995) 19.

[17] S. Padilla, R. Garc´ıa-Carrodeguas, M. Vallet-Reg´ı, Hydroxyapatite suspensions as a precursors of pieces obtained by gelcasting method, J. Eur. Ceram. Soc. 24 (2004) 2223.

[18] M. Toriyama, Slip casting of mechanochemically synthesized hydroxyapatite, J. Mat. Sc. 30 (1995) 3216-3221

[19] F. Lelievre, D. Bernache-assollant, T. chartier, Influence of powder characteristics on the rheological behaviour of hydroxyapatite slurries, J. Mat. Sc.: materials in Medicine7 (1996) 489-494

[20] E.O.Hall, Proc. Phys. Soc., Ser. B, Vol. 64, pp. 747-753, (1951).

[21] N.J.Petch, J. Iron and Steel Institute, pp. 25-28, May 1953.